

Disentangling structure-dependent antioxidant mechanisms in phenolic polymers by multiparametric EPR analysis

Lucia Panzella,* Gerardino D'Errico,* Giuseppe Vitiello, Marco Perfetti, Maria Laura Alfieri, Alessandra Napolitano and Marco d'Ischia

*panzella@unina.it, gderrico@unina.it

Content

Experimental Section	Pag. 2
Natural phenols used for preparation of the polymers	Pag. 5
UV-visible spectra of polymers obtained from different preparations	Pag. 6
ATR-FTIR spectra of VA, CAT and PYR polymers	Pag. 7
FRAP and NO and superoxide scavenging properties of the phenolic polymers	Pag. 10
Kinetic analysis of DPPH decay	Pag. 11
EPR spectra of representative polymers	Pag. 13
Correlations between the results of all the antioxidant assays and EPR parameters	Pag. 14
Determination of the lineshape	Pag. 16
Power saturation profiles of phenolic polymers	Pag. 17
Correlation between antioxidant activity of the phenolic polymers and absorbance at 600 nm	Pag. 18
UV-visible spectra of phenolic polymers	Pag. 19
Effect of hydration on EPR parameters	Pag. 20
EPR analysis using a EMXnano-instrument: comparison with X-band Elexys E-500 results	Pag. 22
References	Pag. 24

Experimental Section

Materials

Horseradish peroxidase (EC 1.11.1.7) (HRP), hydrogen peroxide (30% v/v water solution), 2,2-diphenyl-1-picrylhydrazyl (DPPH), 6-hydroxy-2,5,7,8-tetramethylchromane-2-carboxylic acid (Trolox®), 2,4,6-tri(2-pyridyl)-s-triazine (TPTZ), ferric chloride hexahydrate, linoleic acid, 2,2'-azobis(2-amidinopropane) dihydrochloride (AAPH), Triton X-100, sodium nitroprusside, *N*-(1-naphthylethylenediamine) dihydrochloride, sulfanilamide, nitro blue tetrazolium (NBT), ethylenediaminetetraacetic acid (EDTA) and all the phenolic compounds were purchased from Sigma-Aldrich and used as obtained.

Methods

UV-vis spectra were recorded on a Hewlett Packard 8453 Agilent spectrophotometer. EPR spectroscopy experiments were carried out by means of X-band (9 GHz) Bruker Elexys E-500 spectrometer equipped with a super-high sensitivity probe head. For selected samples, EPR spectra were also acquired using a compact bench-top EPR spectrometer named EMXnano (Bruker Italia is gratefully acknowledged for providing the opportunity to test this instrument). Attenuated total reflectance (ATR)-FTIR spectra were recorded on a Nicolet 5700 Thermo Fisher Scientific instrument.

Phenolic polymer preparation

A solution of the proper phenol (200-500 mg) in ethanol was added to 0.1 M phosphate buffer, pH 6.8, containing 1% KCl (10 mM phenol final concentration) (ethanol/buffer ratio= 1:4 v/v). HRP (2 U/mL final concentration) and hydrogen peroxide (20 mM final concentration) were then added in two portions at 1 h interval, and the mixture was allowed to stand at room temperature under vigorous stirring. After 24 h the mixture was acidified to pH 3 with 3 M HCl and stored at 4 °C for 24 h. The polymer that separated was then collected by centrifugation (7500 rpm, 4 °C, 30 min), washing with 0.1 M HCl and freeze-drying. The yields of the polymers obtained from the same substrate showed $\leq 6\%$ variations. The batch-to-batch reproducibility of the synthetic procedure was checked by recording UV-vis spectra of different preparations of the same polymer (see pag. 6 for representative examples).

DPPH assay¹

30-360 μ L of a 0.33 mg/mL polymer or Trolox solution in DMSO were added to 2 mL of a freshly prepared 0.2 mM solution of DPPH in ethanol; the mixture was taken under vigorous stirring at room temperature and the absorbance at 515 nm was periodically measured over 10 min. Experiments were run in triplicate. Data are expressed as EC₅₀, that is the concentration of the sample at which a 50% DPPH reduction is observed. Kinetic analysis was performed with polymers or Trolox at 8 μ g/mL

FRAP assay²

5-500 μ L of a 0.33 mg/mL polymer or Trolox solution in DMSO were added to 3.6 mL of a 1.7 mM FeCl₃ and 0.83 mM TPTZ in 0.3 M acetate buffer (pH 3.6); the mixture was taken under vigorous stirring

at room temperature and after 10 min the absorbance at 593 nm was measured. Experiments were run in triplicate.

AAPH-induced lipid peroxidation inhibition (LP) assay³

Linoleic acid (0.025 mL) was added dropwise to 0.5 mL of 0.05 M borate buffer, pH 9.0, containing 0.025 mL of Triton X-100. The resulting dispersion was clarified by adding 0.1 mL of 1 M NaOH. The volume was adjusted to 5 mL with additional borate buffer. The resulting linoleic acid solution (16 mM) was stored at 4 °C in the dark until needed. A 40 mM AAPH solution in 0.05 M phosphate buffer, pH 7.4, was freshly prepared.

30 µL of the linoleic acid solution were added to 2.80 mL of 0.05 M phosphate buffer, pH 7.4, pre-thermostated at 37 °C. The oxidation reaction was initiated at 37 °C under air by the addition of 150 µL of the AAPH solution. Oxidation was carried out in the presence of different amounts (0-150 µL) of a 0.33 mg/mL polymer or Trolox solution in DMSO and the increase in absorption at 234 nm was periodically determined. AAPH absorbance in the absence of linoleic acid but in the presence of the polymer was subtracted from each experimental point. Experiments were run in triplicate. Data were expressed as EC₅₀, that is the concentration of the sample at which a 50% reduction of absorption at 234 nm is observed.

NO scavenging assay⁴

600 µL of a 0.33 mg/mL polymer or quercetin solution in DMSO were added to 6 mL of a freshly prepared 10 mM solution of sodium nitroprusside in 0.2 M phosphate buffer (pH 7.4) and the mixture was taken under vigorous stirring at room temperature. After 2 h, 1 mL of the mixture was withdrawn and added to 2 mL of Griess reagent (0.5% sulfanilamide and 0.05% *N*-(1-naphthylethylenediamine) dihydrochloride in 2.5% phosphoric acid) and the absorbance at 540 nm was measured. Results were expressed as percentage of reduction of the absorbance at 540 nm of a control mixture run in the absence of sample. Experiments were run in triplicate.

Superoxide scavenging assay⁵

To 1.6 mL of a 0.5 mM EDTA solution in 0.05 M ammonium hydrogen carbonate buffer (pH 9.3) 400 µL of a 300 µM NBT solution in the same buffer and 100 µL of a 0.33 mg/mL polymer or quercetin solution in DMSO were added, followed by 400 µL of a 20 mM pyrogallol solution in 0.05 mM HCl. The mixture was taken under vigorous stirring and after 5 min the absorbance at 596 nm was measured. Results were expressed as percentage of reduction of the absorbance at 596 nm of a control mixture run in the absence of sample. Experiments were run in triplicate.

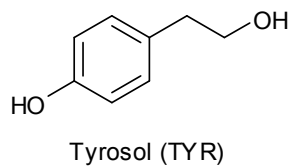
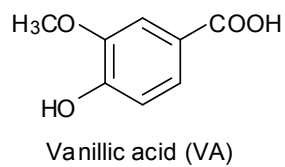
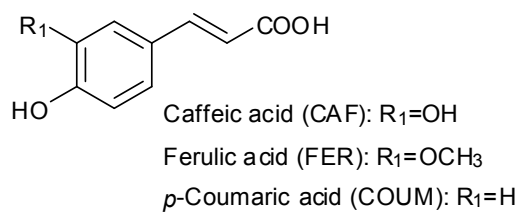
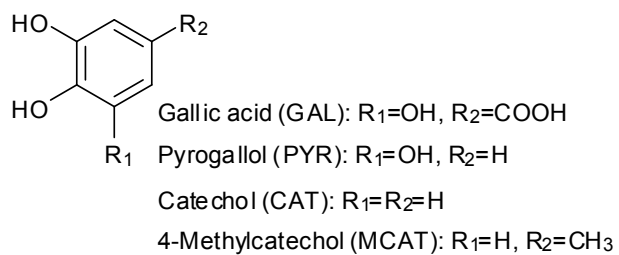
UV-vis spectral characterization of the phenolic polymers

0.33 mg/mL polymer solutions in DMSO were diluted in methanol to a final concentration of 0.01 mg/mL and UV-vis spectra were recorded in the range 200-800 nm.

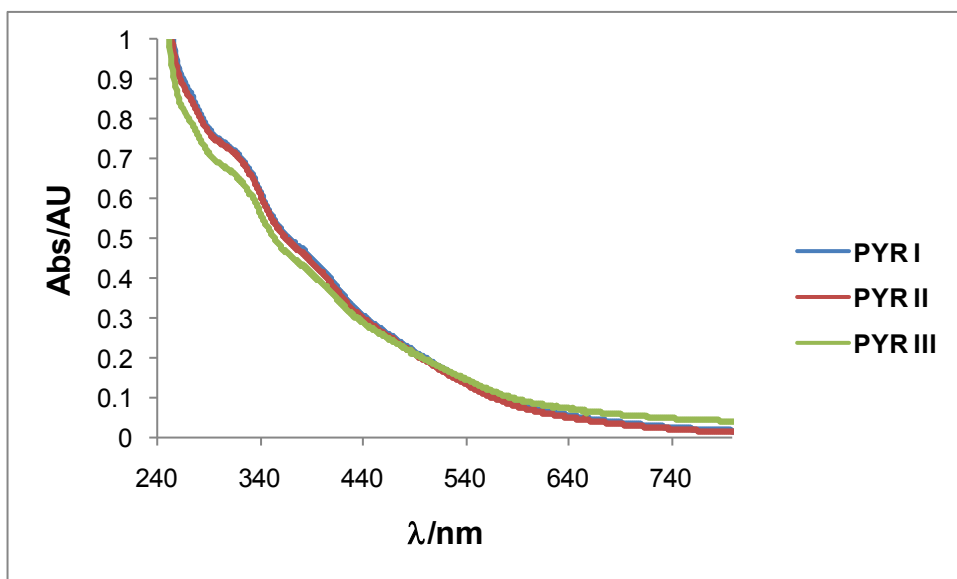
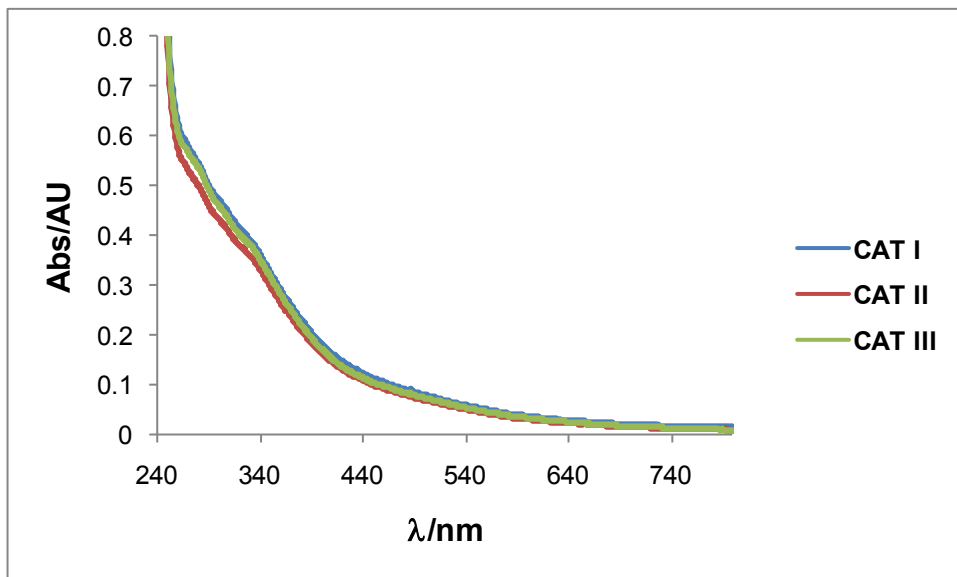
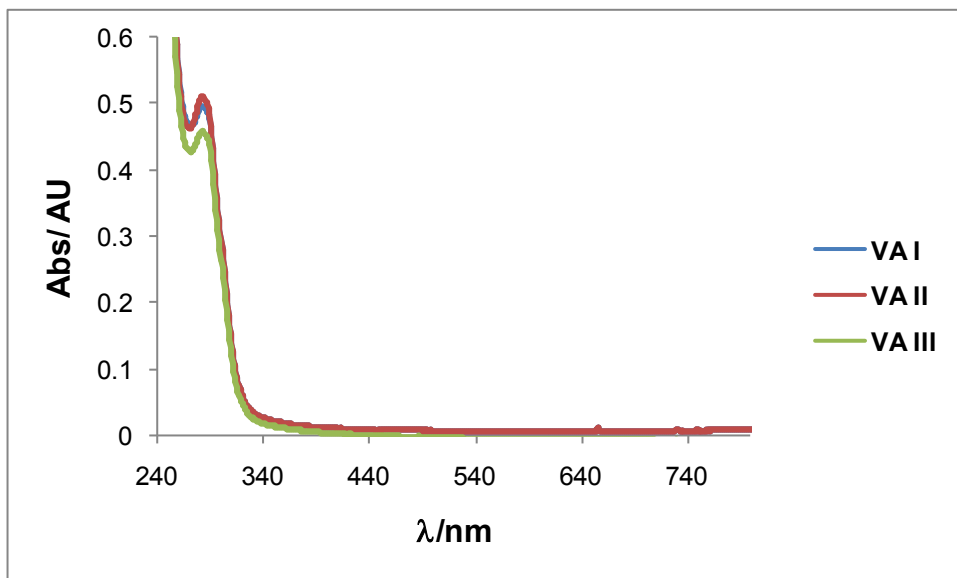
EPR spectral characterization of the phenolic polymers

Samples were transferred to flame-sealed glass capillaries which, in turn, were coaxially inserted in a standard 4 mm quartz sample tube. Measurements performed on the Elexys E-500 spectrometer were run at room temperature. The instrumental settings were as follows: sweep width, 100 G; resolution, 1024 points; modulation frequency, 100 kHz; modulation amplitude, 1.0 G. The amplitude of the field modulation was preventively checked to be low enough to avoid detectable signal overmodulation. The *g*-factor value was evaluated by means an internal standard (Mg/MnO) which was inserted in the quartz sample tube co-axially with the capillary containing the samples.⁶ Power saturation curves were registered by varying the microwave power from about 0.004 mW to about 128 mW. For each sample, 16 different spectra corresponding to distinct values of incident powers were collected. In some cases, at very low powers, the signal intensity was too weak to be distinguished from the spectrum noise, thus it was not taken into account. As a control, spectra of representative polymers were obtained also on hydrated samples and in methanol dispersions, displaying features reflecting those of the spectra from solid samples (Table S1). Also, the experiments were performed by using both a high-level research dedicated instrument and an innovative low-cost bench-top equipment, obtaining superimposable results (Table S2 and S3).

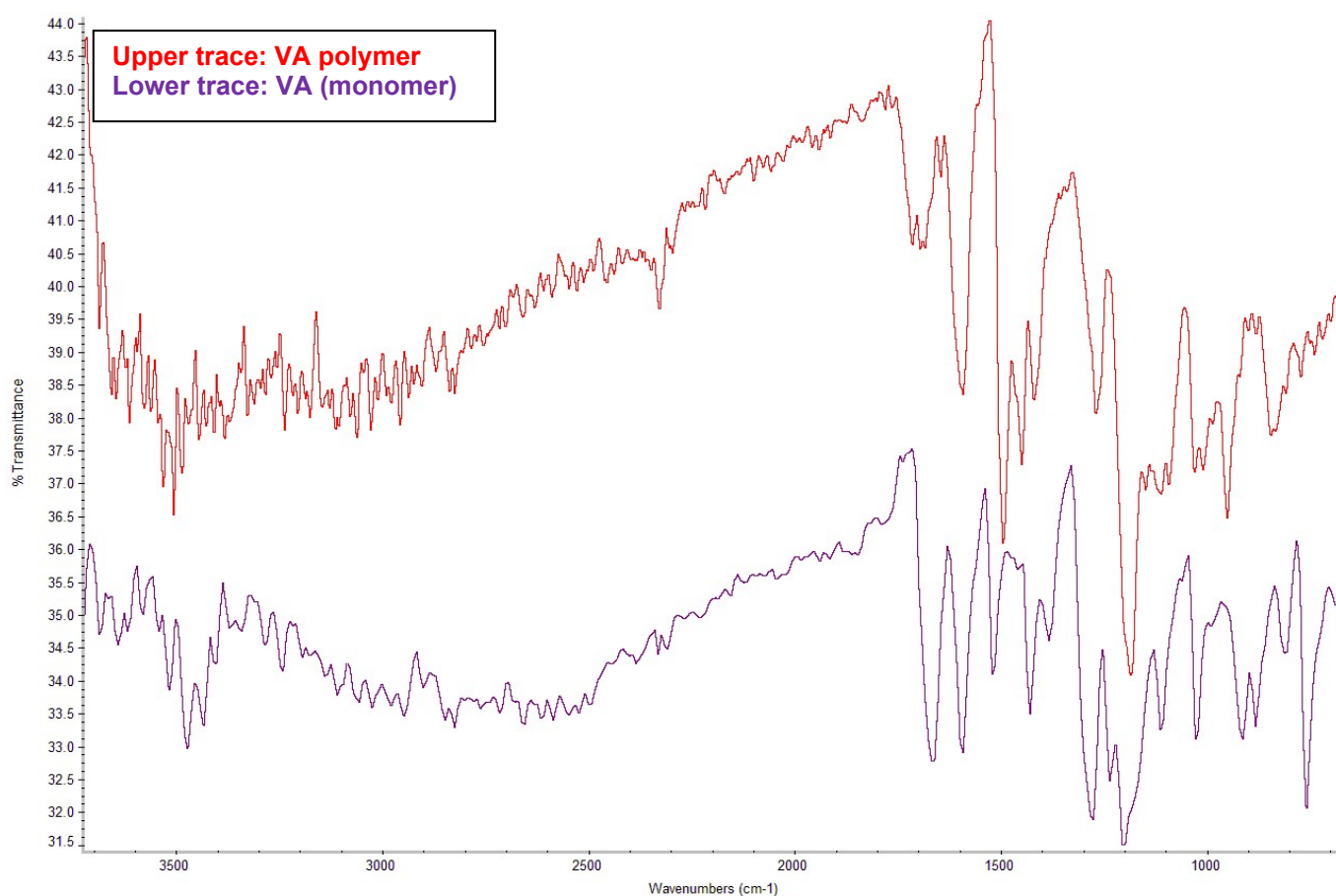
Natural phenols used for preparation of the polymers



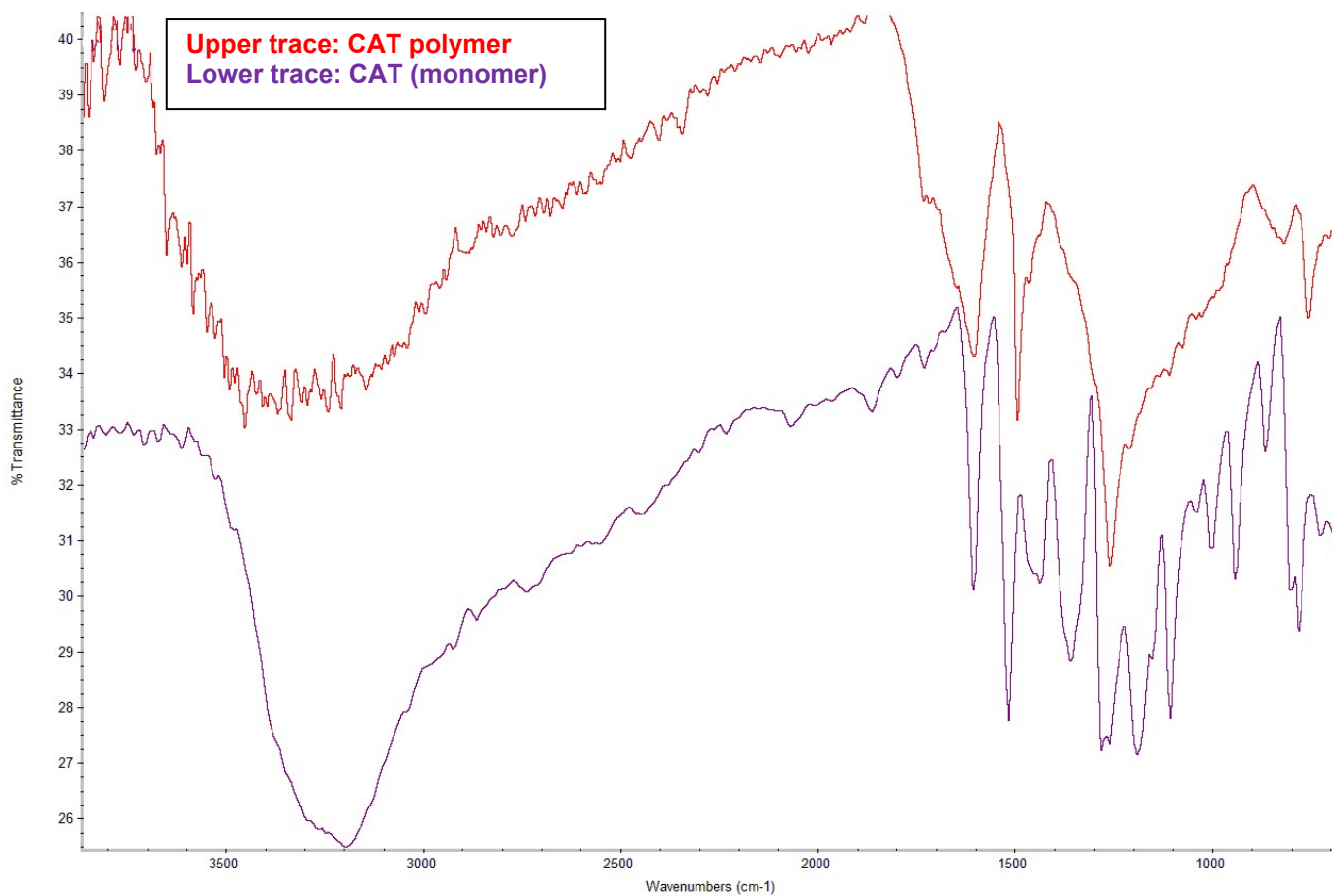
UV-visible spectra of VA, CAT and PYR polymers obtained from three different preparations



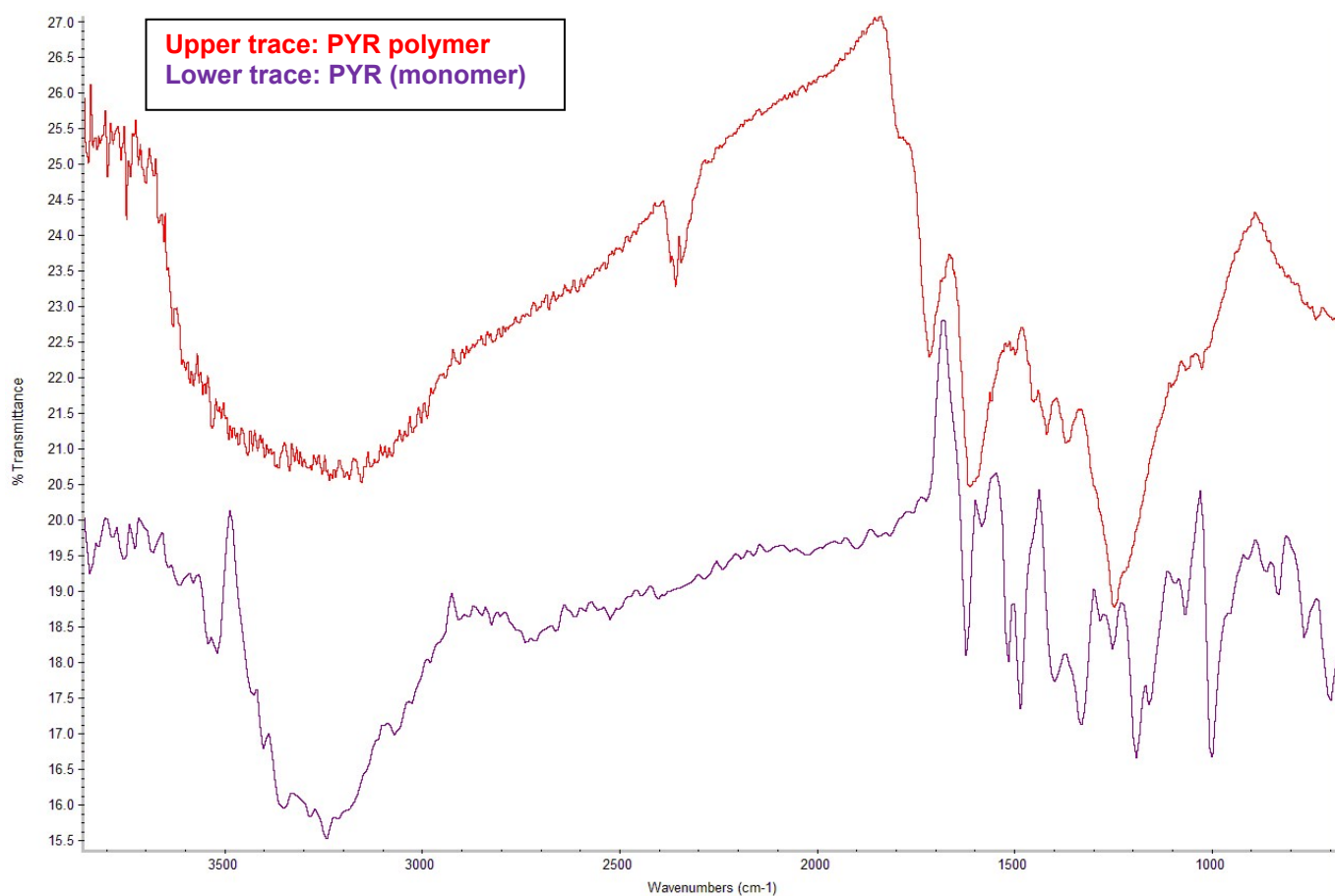
ATR-FTIR spectra of VA, CAT and PYR polymers



The bands at ca. 1660 and 1270 cm^{-1} due to the C=O stretching and O-H bending vibration of the carboxylic group were greatly reduced in the spectrum of the polymer, suggesting extensive decarboxylation of VA during the oxidation process. Polymerization was also responsible for the almost complete disappearance of the C-H bending band at ca. 750 cm^{-1} .

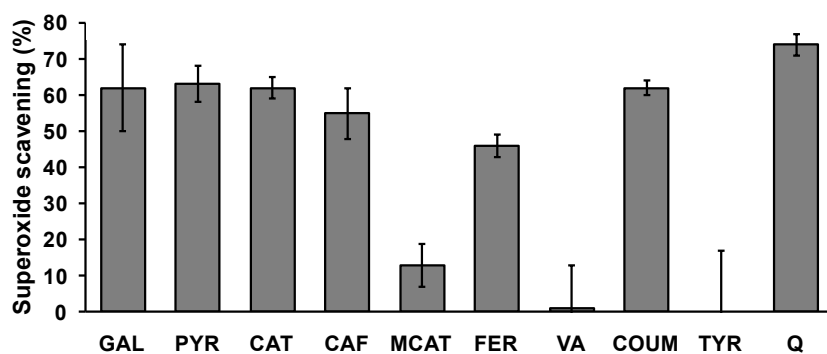
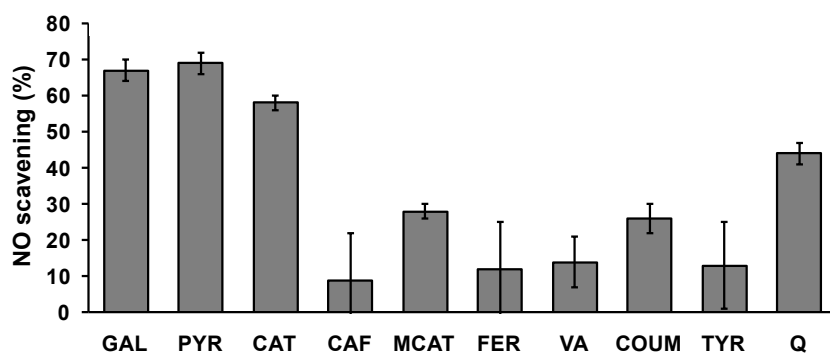
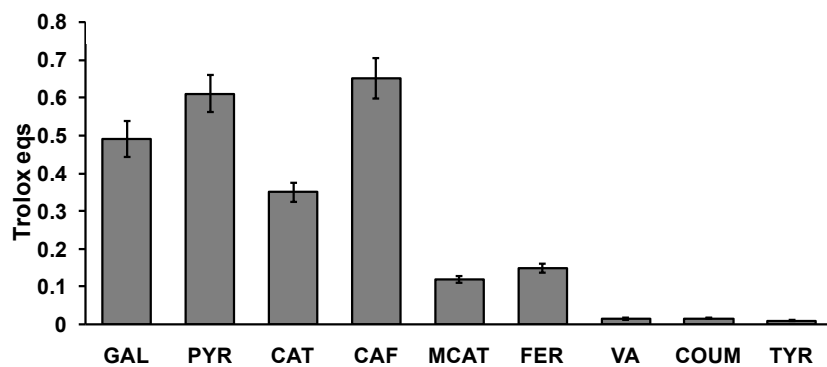


A slight decrease and shift to higher frequencies were observed for the O-H stretching band in the region 3500-3000 cm^{-1} in the case of the polymer. A lower resolution in the region 1500-1100 cm^{-1} was also observed further to CAT oxidation, with only a main band at ca. 1250 cm^{-1} , likely due to C–O–C stretching of phenyl ether moieties arising from polymerization. Finally, a lower intensity of the C-H bending bands at 900-700 cm^{-1} was observed for the polymer.

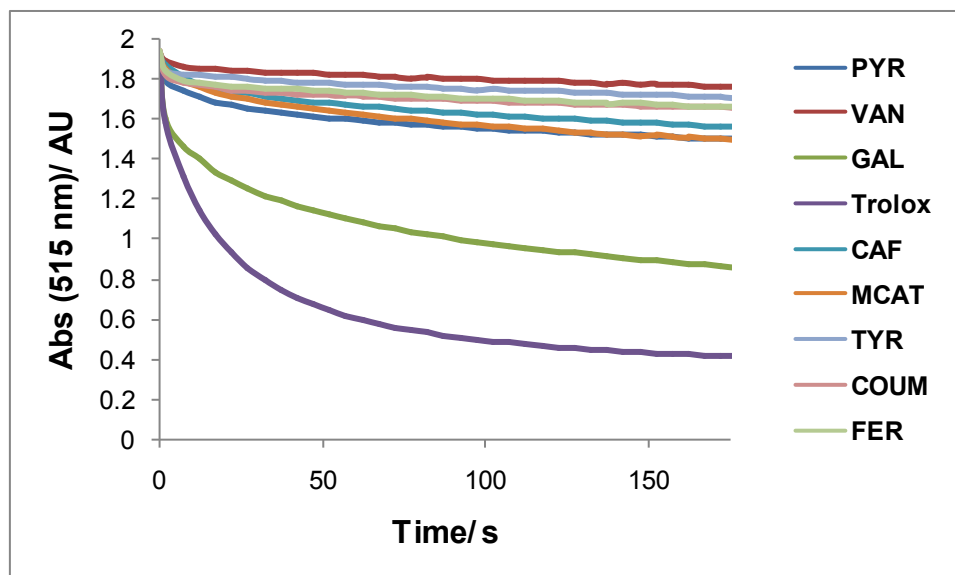


Spectral features characteristic of purpurogallin-like moieties were evident for the PYR polymer, i.e. two bands at ca. 1600 (C=C-C=O stretching) and 1250 (C-O stretching) cm^{-1} .

FRAP (expressed as Trolox eqs) and NO and superoxide scavenging properties of the phenolic polymers (abbreviations refer to the starting monomer). Reported are the mean \pm SD values of at least three experiments. Q= quercetin



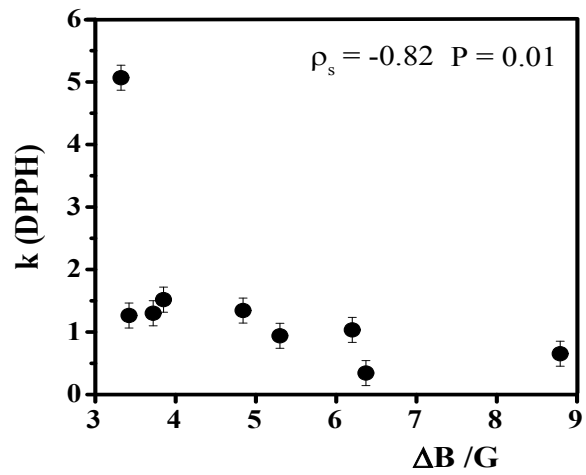
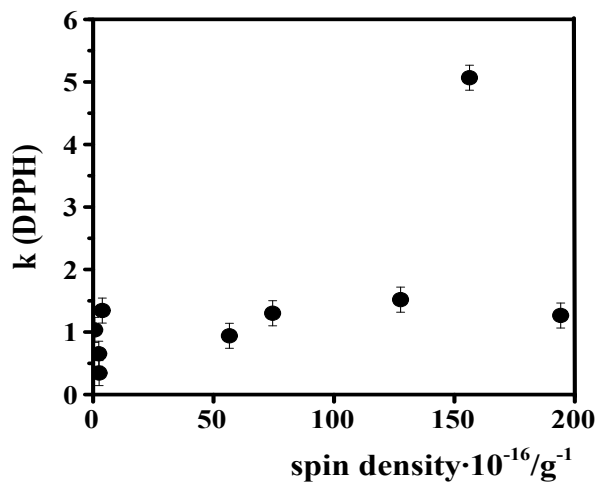
Kinetic analysis of the decay of DPPH (200 μ M starting concentration) absorbance at 515 nm in the presence of 8 μ g/mL phenolic polymers or Trolox.



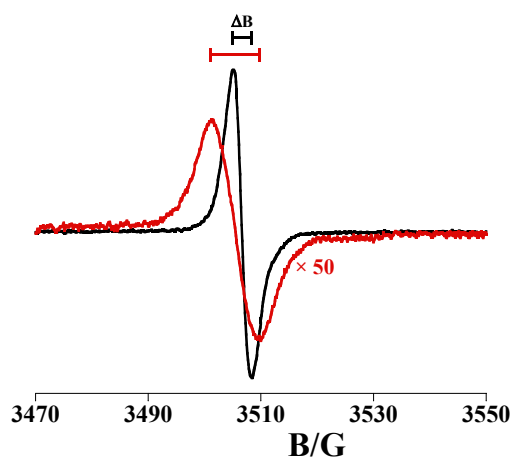
Antioxidant	k ($L g^{-1} s^{-1}$) ^a
GAL	5.1 ± 0.4
PYR	1.5 ± 0.1
CAT	1.26 ± 0.09
CAF	1.4 ± 0.1
MCAT	1.34 ± 0.09
FER	0.94 ± 0.07
VA	0.34 ± 0.02
COUM	1.03 ± 0.07
TYR	0.65 ± 0.05
Trolox	12.5 ± 0.9

^aRate constant for the fast step (mean \pm SD values, n=3).

As apparent from the plots and rate constants reported above, an efficacy trend similar to that determined based on the EC50 values (see main text) was observed, with polymers from tri- and diphenols being most active also from a kinetic point of view. Notably, the polymer from gallic acid proved to be very effective as a DPPH reducing agent, with a rate constant approaching 40% of that determined for the reference antioxidant Trolox. As reported below, a good correlation was found between the rate constants and the ΔB values, but not the spin density values.

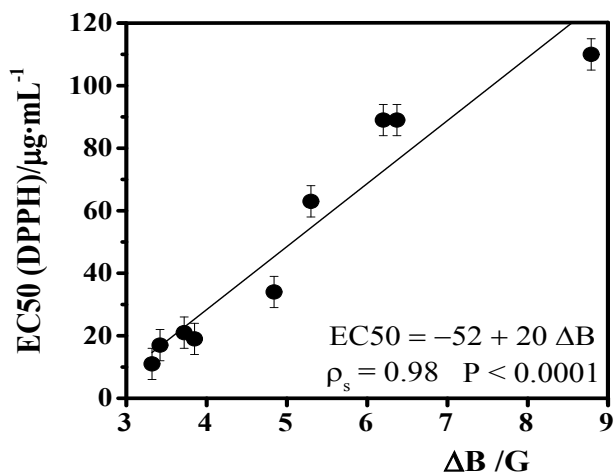
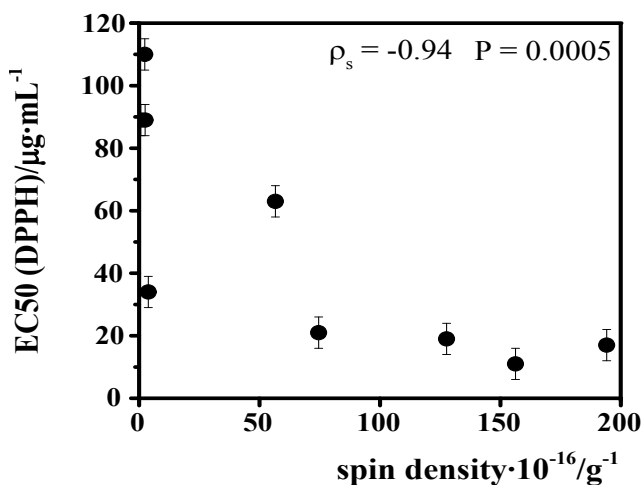


EPR spectra of gallic acid (black) and tyrosol (red) polymers

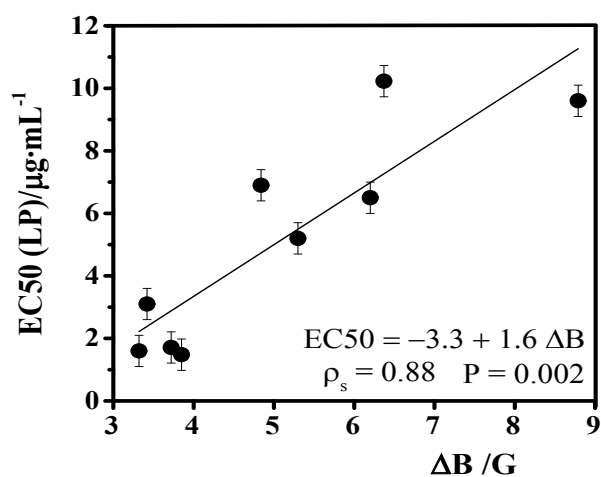
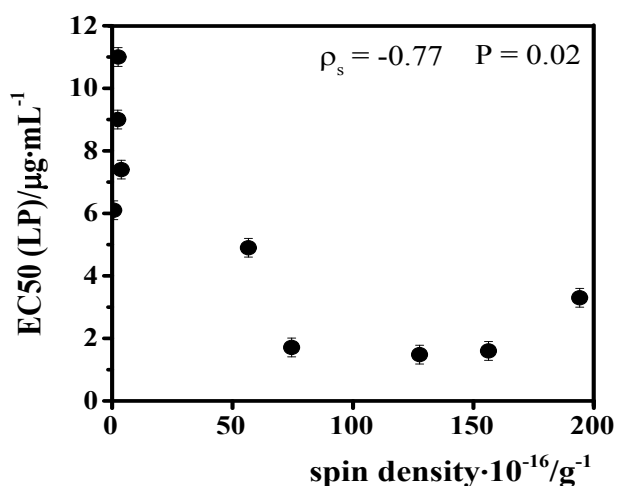


Correlations between the results of all the antioxidant assays and EPR parameters.

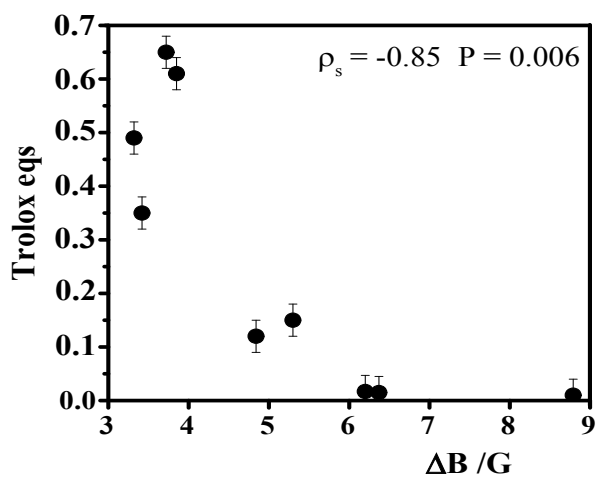
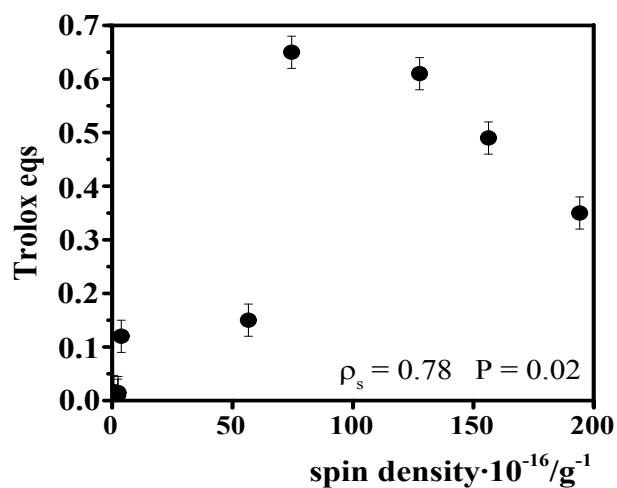
DPPH assay



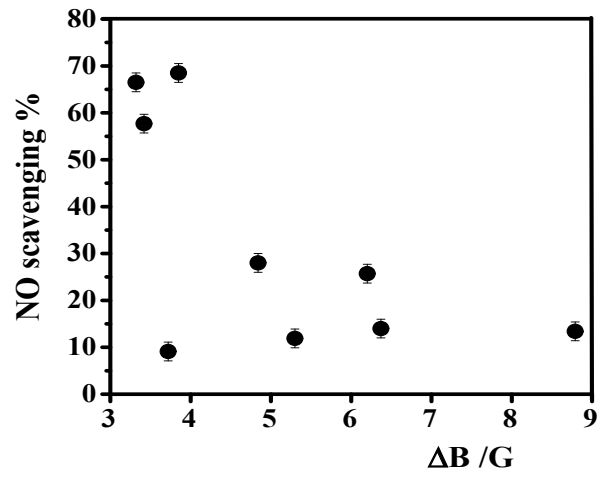
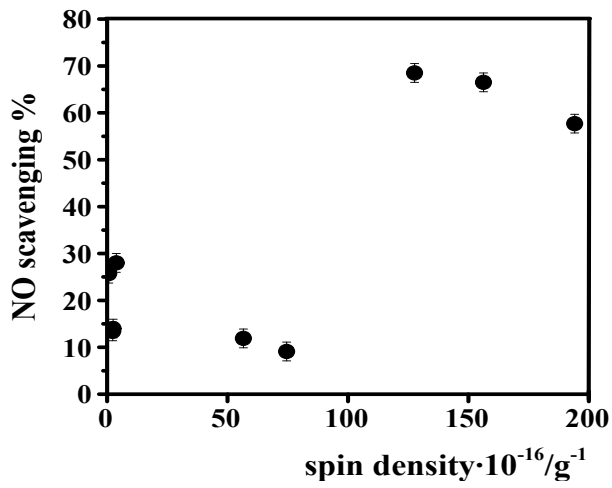
LP assay



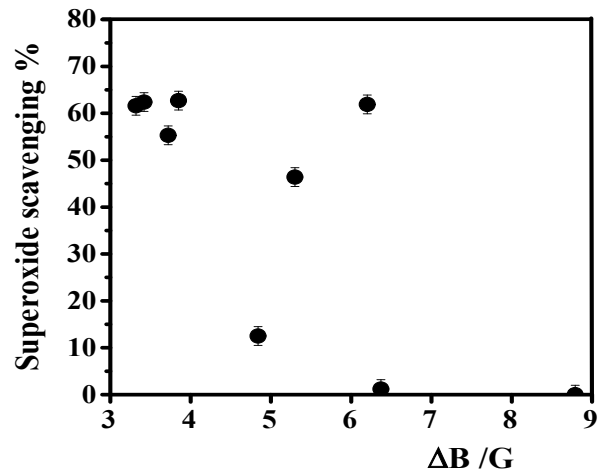
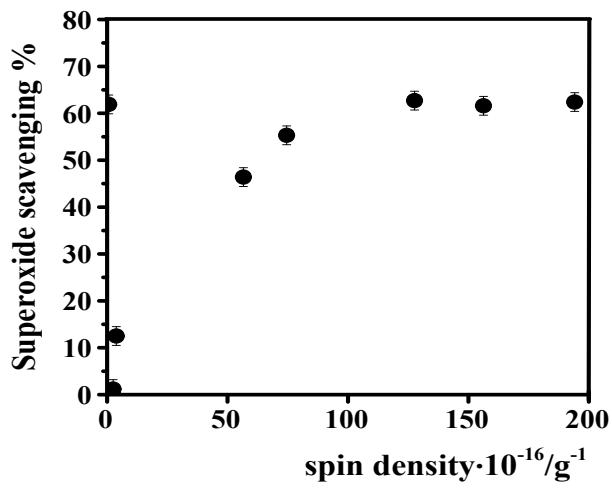
FRAP assay



NO scavenging assay



Superoxide scavenging assay



Determination of the lineshape

Determination of the Gaussian and Lorentzian contributions to the lineshape was obtained by estimating the $\Delta B_{1/2}/\Delta B$ ratio, where $\Delta B_{1/2}$ is the half-height width of the EPR absorption signal and ΔB is the peak-to-peak distance of the first-derivative signal (instrumental output). This ratio is 1.72 for a Lorentzian curve and 1.18 for a Gaussian curve. In all the cases considered in the present work an intermediate value was obtained, from which the percentages of Lorentzian character of the lineshape was estimated.⁷

Power saturation profiles of the phenolic polymers

The power saturation profiles of the EPR signal from the phenolic polymers are reported in Figure S1. A homogeneous saturation trend was observed for catechol, 4-methylcatechol, pyrogallol, gallic acid, tyrosol and vanillic acid polymers, whereas a heterogeneous saturation was found for the cinnamic acid (caffeic, ferulic and *p*-coumaric acid) polymers.

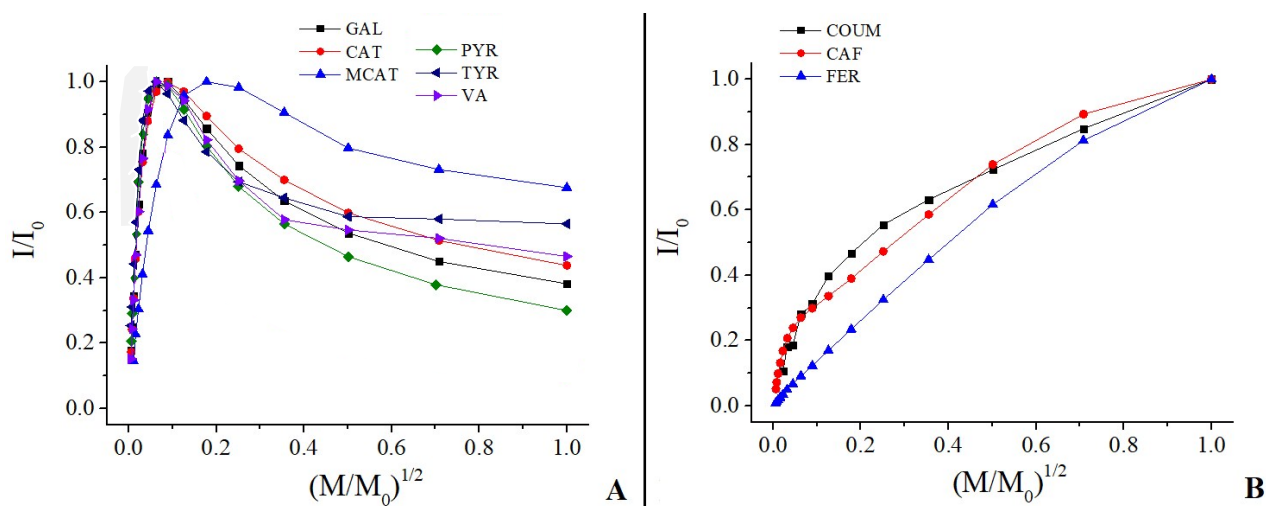
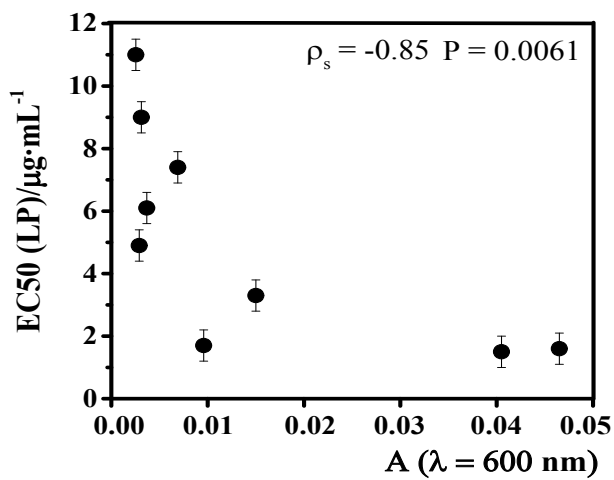
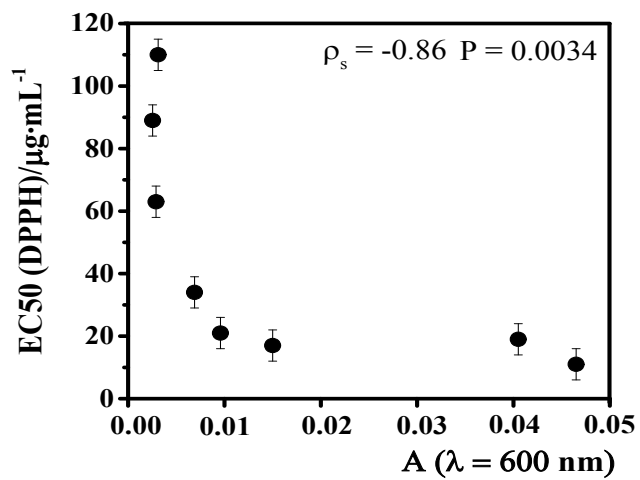
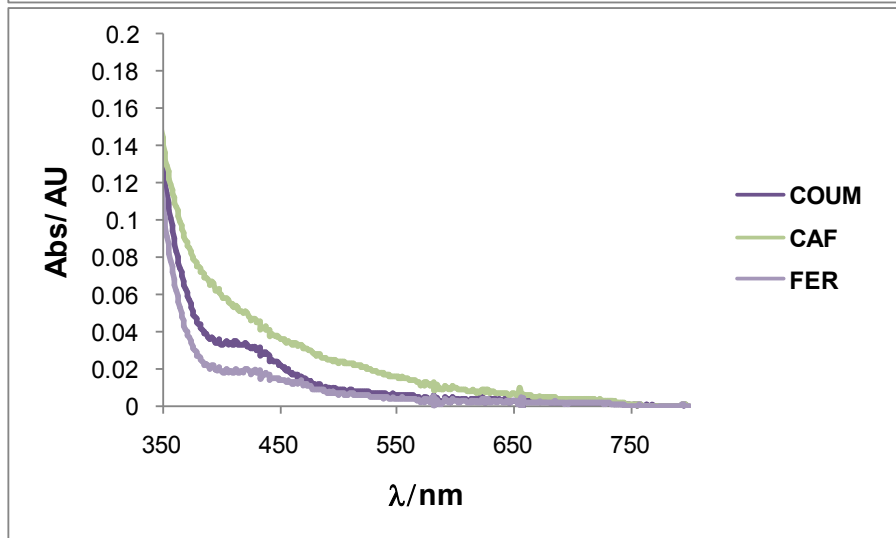
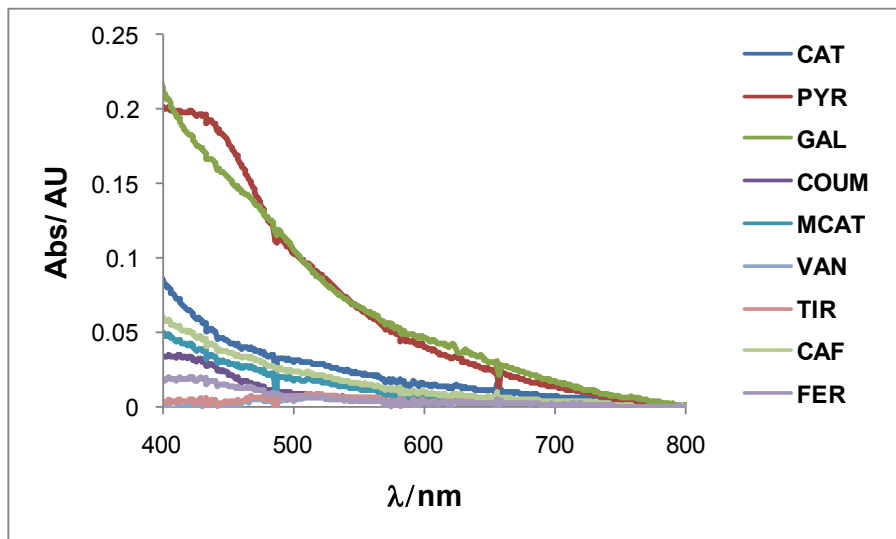
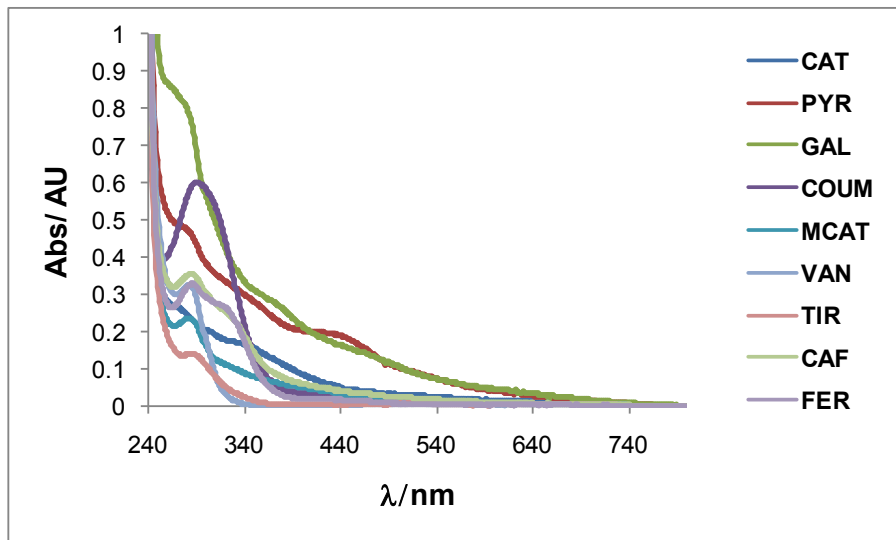


Figure S1 - Power saturation profiles for all investigated phenolic polymers showing a homogeneous trend (panel A) and a heterogeneous trend (panel B).

Correlation between antioxidant activity of the phenolic polymers (expressed as the EC50 values determined in the DPPH and LP assays) and absorption in the visible range (determined at $\lambda = 600$ nm).



UV-visible spectra of the phenolic polymers (0.01 mg/mL methanolic solution) (*top panel: 240-800 nm range; middle panel: visible range (400-800 nm); bottom panels: spectra of hydroxycinnamic acid polymers*).



Of the three polymers from hydroxycinnamic acids (CAF, FER and COUM) only that from CAF, the most active in the DPPH, LP and FRAP assays, exhibited significant absorption at 600 nm.

Effect of hydration on EPR parameters

In order to study the effect of hydration on the paramagnetic properties of the investigated phenolic polymers, we also carried out EPR measurements on aqueous dispersions. However, the intensity of the signal was too low to be reliably analyzed. Therefore, we performed an EPR study on the hydrated powders of polymers from pyrogallol and *p*-coumaric acid, showing a distinct behavior in terms of ΔB , spin-density and saturation profile. Dry powders from both polymers were hydrated for 15 h in a saturated atmosphere at room temperature. Then, the hydrated samples were characterized by EPR. Afterwards, samples were dried under vacuum in the presence of phosphoric anhydride in order to gravimetrically check the hydration degree, which was found to be about 50%. Finally, EPR analysis on dried samples was carried out.

The parameters derived from the spectra are shown in Table S1. Overall the hydration effects were weak, and did not affect the relative comparison between the two polymers, thus fully supporting the use of the data determined from the spectra of solid samples obtained by freeze-drying, presented in the main text. In details, spin-density of pyrogallol polymer slightly decreased upon hydration, while in the case of *p*-coumaric acid this parameter was poorly affected by hydration and dehydration treatments. A slight decrease of the *g*-factor was observed for the hydrated samples. For *p*-coumaric acid polymer, hydration resulted in a decrease of the ΔB parameter, which however remained quite high.

Table S1 – Spin-density, *g*-value and ΔB for not hydrated, hydrated and dried samples.

monomer precursor	Spin-density (spin/g)	ΔB (G)	<i>g</i> -factor
PYR (before hydration)	1×10^{18}	3.8	2.0033
PYR (hydrated)	6×10^{17}	3.9	2.0028
PYR (dried)	9×10^{17}	3.8	2.0033
PYR (methanol)	7×10^{17}	4.0	2.0031
COUM (before hydration)	7×10^{15}	6.2	2.0031
COUM (hydrated)	6×10^{15}	5.6	2.0027
COUM (dried)	5×10^{15}	6.0	2.0030
COUM (methanol)	5×10^{15}	5.9	2.0030

Figure S2 reports the power saturation profile comparison between hydrated and dried (i.e. dehydrated) polymers, as well as between samples before and after the hydration treatment. It is worth noting that for *p*-coumaric acid polymer both the hydrated and the dried sample showed a heterogeneous behavior, whereas for pyrogallol the saturation was heterogeneous for the hydrated sample and homogeneous for the sample before hydration. Therefore, in the case of pyrogallol polymer the hydration significantly influenced the spin distribution. However, the drying process switched back the pyrogallol polymer to an homogeneous behavior.

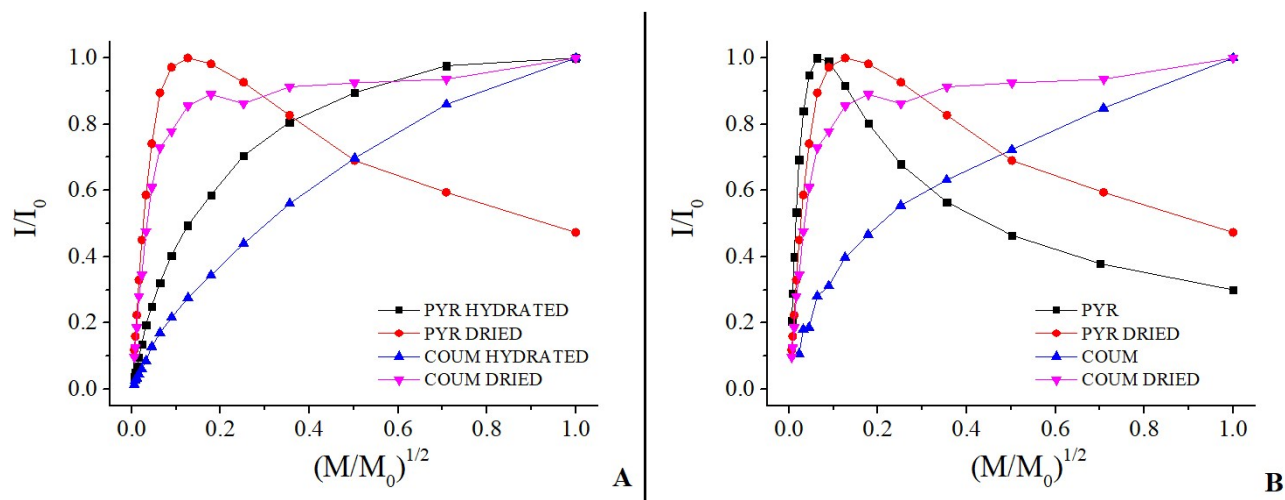


Figure S2 - Power saturation profiles for pyrogallol and *p*-coumaric acid polymers: comparison among hydrated and dried (i.e. dehydrated) species (panel **A**) and among not hydrated and dried species (panel **B**).

We also analyzed the same two phenolic polymers finely dispersed in methanol. This test is interesting since some tests of antioxidant activity are run in methanol. The data, shown in Table S1, indicated that this solvent did not significantly affect the radical behavior of the polymers as detected by EPR.

EPR analysis using a EMXnano-instrument: comparison with X-band Elexys E-500 results

For a selection of samples, the same EPR analysis was carried out by using a different instrument, a compact bench-top EPR spectrometer named EMXnano. Spin density, g value and ΔB were evaluated and shown in Table S2. It is to be highlighted that in the case of EMXnano, g -factors were calculated by using an internal marker of the instrument. The values obtained with the two instruments were in very good agreement.

Table S2 - Spin-density, g -value and ΔB obtained from X-band Elexys E-500 and EMXnano spectrometers for three different phenolic polymers

monomer precursor	Spin-density (spin/g)		ΔB (G)		g -factor	
	Elexys	EMX	Elexys	EMX	Elexys	EMX
VA	2.5×10^{16}	3.5×10^{16}	6.4	6.6	2.0028	2.0031
MCAT	3.8×10^{16}	4.2×10^{16}	4.8	5.1	2.0033	2.0035
TYR	2.4×10^{16}	1.8×10^{16}	8.8	8.9	2.0033	2.0034

Power saturation profile for 4-methylcatechol polymer was determined by the EMXnano and compared to that collected by using the X-band Elexys E-500. Figure S3 reports the comparison of the power saturation profiles from both instrument and shows a perfect overlap between the two curves. Also the normalized power value at which the signal saturation is reached is the same. Therefore, the use of a compact, relatively low-cost, bench-top spectrometer allows obtaining reliable EPR data which can be perfectly compared to the ones got from a more powerful instrument. This opens to a wider diffusion of EPR spectroscopy as a basic characterization of materials containing unpaired electrons or participating to radical processes.

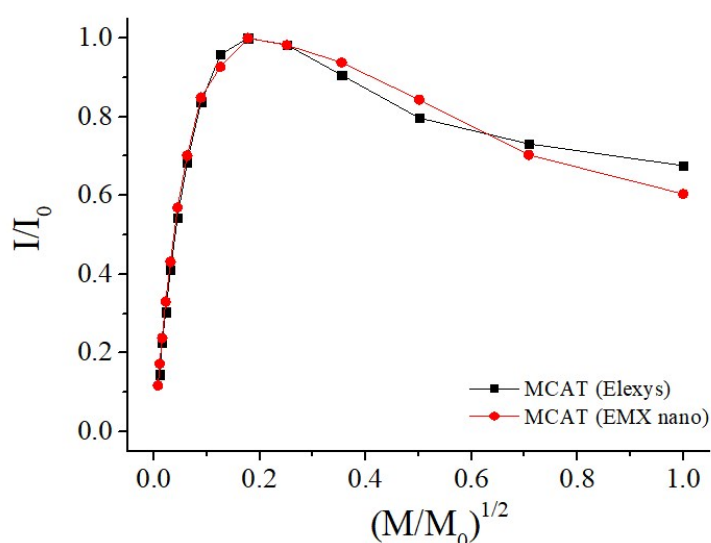


Figure S3 – Power saturation profiles for 4-methylcatechol polymer obtained by using a X-band Elexys E-500 spectrometer and the compact EMXnano spectrometer.

EMXnano instrument also allowed performing measurements at low temperatures. In particular, we were interested in investigating the changes of spin density, g-factor and ΔB with temperature. Therefore, spectra of 4-methylcatechol polymer were collected at 298 K and 120 K by using the same acquisition parameters. Measurements were performed in the presence and in the absence of the internal marker included in the instrument. The comparison between the spectral parameters is shown in Table S3, showing an overall good agreement. A slight increase of the ΔB parameter was observed at lower temperatures, which can be associated to a slower mobility of the radicals that results in a shorter relaxation time. Moreover, the low value of g-factor confirmed the presence of pure carbon-centered radicals.

Table S3 - Spin-density, g-value and ΔB obtained at different temperatures from EMXnano spectrometer for 4-methylcatechol polymer.

monomer precursor	Spin-density (spin/g)		ΔB (G)		g-factor	
	120 K	298 K	120 K	298 K	120 K	298 K
MCA	7.4×10^{16}	4.4×10^{16}	6.90	6.03	2.0029	2.0035

References

1. P. Goupy, C. Dufour, M. Loonis and O. Dangles, *J. Agric. Food Chem.*, 2003, **51**, 615-622.
2. I. F. F. Benzie and J. J. Strain, *Anal. Biochem.*, 1996, **239**, 70-76.
3. C. Liégeois, G. Lermusieau and S. Collin, *J. Agric. Food Chem.*, 2000, **48**, 1129-1134.
4. L. Marcocci, J. J. Maguire, M. T. Droy-Lefaix and L. Packer, *Biochem. Biophys Res. Commun.*, 1994, **201**, 748-755.
5. C. Xu, S. Liu, Z. Liu, F. Song and S. Liu, *Anal. Chim. Acta*, 2013, **793**, 53-60.
6. F. Sannino, P. Pernice, C. Imparato, A. Aronne, G. D'Errico, L. Minieri, M. Perfetti and D. Pirozzi, *RSC Adv.*, 2015, **5**, 93831–93839.
7. A. G. Requejo, N. R. Gray, H. Freund, H. Thomann, M. T. Melchior, L. A. Gebhard, M. Bernardo, C. F. Pictroski and C. S. Hsu, *Energy Fuels*, 1992, **6**, 203-214.